AFRL-OSR-VA-TR-2015-0156

Self Assembly and Pyroelectric Poling for Organics

Alex K Y Jen
UNIVERSITY OF WASHINGTON

07/06/2015
Final Report

Air Force Research Laboratory
AF Office Of Scientific Research (AFOSR)/ RTD
Arlington, Virginia 22203
Air Force Materiel Command

REPORT DOCUMENTATION PAGE

Form Approved
OMB No. 0704-0188

1. REPORT DATE *(DD-MM-YYYY)*	2. REPORT TYPE	3. DATES COVERED *(From - To)*
14-07-2015	Final Performance	01-04-2012 to 31-03-2015

4. TITLE AND SUBTITLE
Multifunctional Self-Assembled Molecular Materials for Monolayer Field-Effect and Photo-Transistors

5a. CONTRACT NUMBER

5b. GRANT NUMBER
FA9550-12-1-0076

5c. PROGRAM ELEMENT NUMBER

6. AUTHOR(S)
Alex K Y Jen

5d. PROJECT NUMBER

5e. TASK NUMBER

5f. WORK UNIT NUMBER

7. PERFORMING ORGANIZATION NAME(S) AND ADDRESS(ES)
UNIVERSITY OF WASHINGTON
4333 BROOKLYN AVE NE
SEATTLE, WA 981950001 US

8. PERFORMING ORGANIZATION REPORT NUMBER

9. SPONSORING/MONITORING AGENCY NAME(S) AND ADDRESS(ES)
AF Office of Scientific Research
875 N. Randolph St. Room 3112
Arlington, VA 22203

10. SPONSOR/MONITOR'S ACRONYM(S)
AFOSR

11. SPONSOR/MONITOR'S REPORT NUMBER(S)

12. DISTRIBUTION/AVAILABILITY STATEMENT
A DISTRIBUTION UNLIMITED: PB Public Release

13. SUPPLEMENTARY NOTES

14. ABSTRACT
Insulating, dipolar and semiconducting molecular phosphonic acid (PA) self-assembled monolayers (SAMs) have been developed for applications in organic field-effect transistors (OFETs) and graphene transistors for low-power, low-cost flexible electronics. Multifunctional SAMs on ultrathin metal oxides, such as hafnium oxide and aluminum oxide, are shown to realize (1) enhanced performance of self-assembled monolayer field-effect transistors (SAMFETs) , (2) bottom-contact small-molecule n-type organic field effect transistors , (3) low operational voltage and high performance organic field effect memory transistors , and (4) systematic doping control of CVD graphene transistors. Key strategies of using electric field generated by pyroelectricity have been explored to efficiently pole highly efficient organic electro-optic (OEO) materials in thin films and nanophotonic waveguides. Through surface modification, novel pyroelectric elements such as pyroelectric crystals and ceramics are modified as conformal and detachable electric field source to study basic electrostatics and develop new device concepts for hybrid OEO nanophotonic platforms.

15. SUBJECT TERMS
pyroelectric, poling of EO polymers, electrooptic polymers

16. SECURITY CLASSIFICATION OF:			17. LIMITATION OF ABSTRACT	18. NUMBER OF PAGES	19a. NAME OF RESPONSIBLE PERSON
a. REPORT	b. ABSTRACT	c. THIS PAGE			Alex K Y Jen
U	U	U	UU		19b. TELEPHONE NUMBER *(Include area code)* 206-543-2626

Standard Form 298 (Rev. 8/98)
Prescribed by ANSI Std. Z39.18

Final Report

To: technicalreports@afosr.af.mil
Subject: Final Report to Dr. Charles Lee

PI: Alex K.-Y. Jen
Contract/Grant Title: Self Assembly and Pyroelectric Poling for Organics
Contract/Grant #: FA9550-12-1-0076
Reporting Period: 4/1/12 – 3/31/15

Section 1: Multifunctional Self-Assembled Molecular Materials for Monolayer Field-Effect and Photo-Transistors

Executive Summary

Insulating, dipolar and semiconducting molecular phosphonic acid (PA) self-assembled monolayers (SAMs) have been developed for applications in organic field-effect transistors (OFETs) and graphene transistors for low-power, low-cost flexible electronics. Multifunctional SAMs on ultrathin metal oxides, such as hafnium oxide and aluminum oxide, are shown to realize (1) enhanced performance of self-assembled monolayer field-effect transistors (SAMFETs) with top-contact geometry through molecular tailoring, heated assembly and thermal annealing, (2) bottom-contact small-molecule n-type organic field effect transistors achieved via simultaneous modification of electrode and dielectric surfaces, (3) understanding of effects from self-assembled monolayer structural order, surface homogeneity and surface energy on pentacene morphology and thin film transistor device performance, (4) low operational voltage and high performance organic field effect memory transistors with solution processed graphene oxide charge storage media, and (5) systematic doping control of CVD graphene transistors with functionalized self-assembled monolayers.

1. Enhanced performance of self-assembled monolayer field-effect transistors with top-contact geometry through molecular tailoring, heated assembly and thermal annealing

Self-assembled monolayer field-effect transistors are a promising concept that uses rationally designed π-conjugated SAMs as the semiconductor of a transistor. This concept works in principle because charge transport in an organic semiconductor based FET occurs in the first few monolayers closest to the dielectric. SAMFETs are believed to have a broad appeal for organic semiconductor applications due to their low-cost processing, reduced material quantity needed compared to traditional organic thin film transistors and ability to be used toward flexible electronics and sensing applications.

High performance low operating voltage SAMFETs have been fabricated through the rational design of a functional SAM head group and processing optimization (Fig. 1). The methylthiobutyl terminal group of the quaterthiophene based SAM semiconductors has enabled efficient electrical contact to Au electrodes while maintaining SAMFET thermal stability. Annealing has been shown to further enhance the coordinate bond between SAM and electrode to enable over two orders of magnitude increase in charge carrier mobility. Additionally, through the use of heated immersion assembly, SAM density has been increased by approximately 30% resulting in another order of magnitude higher charge carrier mobility. Low voltage SAMFETs utilizing hybrid HfO_2 sol-gel dielectric were then assembled under optimized processing conditions to achieve a peak hole-mobility of 0.015 $cm^2\ V^{-1}\ s^{-1}$. These results show the importance of terminal group and processing for SAMFETs and should be generally applicable to other SAM semiconductor systems.

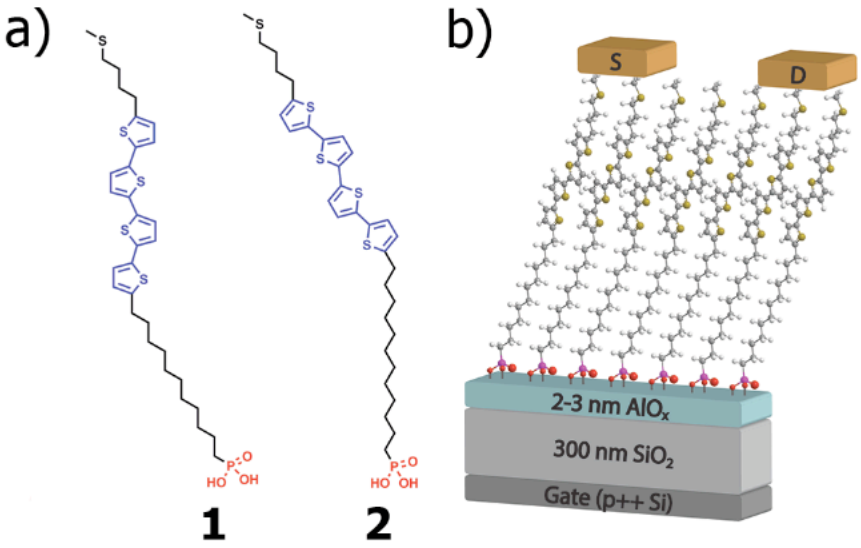

Fig. 1. (a) Molecular structures of SAM semiconductors, **1** MTB4TC11 and **2** MTB4TC12; (b) schematic of high-voltage SAMFETs fabricated.

2. Bottom-contact small-molecule n-type organic field effect transistors achieved via simultaneous modification of electrode and dielectric surfaces

It has been shown that through a simple spin-cast procedure one is able to simultaneously modify the source/drain metal electrodes and metal oxide dielectric with simple alkyl phosphonic acid SAMs. This dual modification allows for the passivation of surface hydroxyl groups that can act as electron traps at the dielectric interface, a reduction of Frölic polaron formation between charge carriers in the OSCs caused by the SAM acting as a physical buffer against the induced ionic polarization from a high-*k* material used for low-voltage applications as well as reduction of the source/drain contact resistance due to SAM-modified metal/OSC interface. However, alkylphosphonic acid SAMs are not compatible with solution-processable small-molecule OSCs due to the low surface energy of methyl-terminated SAMs which causes limited surface wettability. In particular, soluble small-molecule OSCs, such as [6,6]-phenyl-C_{61}-butyric acid methyl ester (PCBM), are typically unable to form thin films on low surface energy substrates resulting in significantly reduced or no device performance. We have investigated the effect of 6-phenoxylhexylphosphonic acid (Ph6PA) SAM on top- and bottom-contact low-voltage *n*-type organic OFETs (Fig. 2). C_{60} and PCBM were chosen as the semiconductors in order to compare the effect that Ph6PA SAM plays on OFET device performance, morphology, and contact resistance on solution-processed and thermally evaporated small-molecule n-type materials.

Through rational molecular design and process optimization a SAM has been developed to simultaneously modify both source/drain electrodes and metal oxide dielectric surfaces and be compatible with solution processable and thermally evaporated organic semiconductors. Our results show comparable performance between top- and bottom-contact device architectures with an average electron mobility of C_{60} TC and BC devices of 0.212 and 0.320 $cm^2\ V^{-1}\ s^{-1}$ respectively. PCBM devices yielded 0.04 and 0.06 $cm^2\ V^{-1}\ s^{-1}$ for TC and BC devices respectively. Low contact resistance between 11 and 45 kΩ cm was found regardless of device architecture or n-type semiconductor used. Through this simultaneous SAM modification photolithography compatible and solution processed semiconductor-based OFET devices are achievable without being inhibited by the performance degradation that typically accompanies the bottom-contact device architecture.

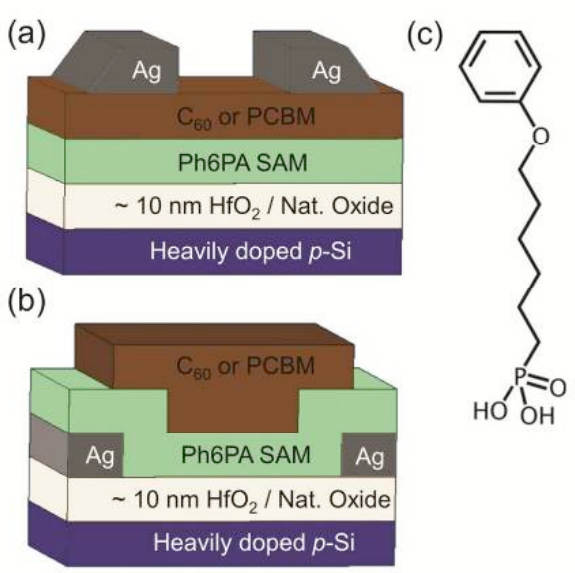

Fig. 2. (a) Top- and (b) bottom-contact bottom-gate device architectures and (c) 6-phenoxyhexylphosphonic acid (Ph6PA) self-assembled monolayer molecule.

3. Effects of self-assembled monolayer structural order, surface homogeneity and surface energy on pentacene morphology and thin film transistor device performance

Great effort has been devoted to exploring the relationship between SAM structure and electronic performance of various commonly used organic semiconducting small molecules/polymers. Mechanisms for improving device performance have included: surface energy, SAM density/phase states, and π-π and/or π-σ interactions. However, these claims are frequently made using a narrow selection of SAM structures, leading to explanations that often correlate semiconductor performance to an observed trend without identifying a causal relationship. Additionally, results are sometimes achieved in conjunction with one or more confounding variables such as a large dielectric surface roughness or molecular aggregate on the SAM surfaces. Due to the breadth of mechanisms observed for SAM structure affecting device performance, our group chose to examine six SAM structures and their impact on pentacene device performance with respect to surface energy, surface homogeneity, and level of structural order; three underlying principles of SAM surface science. SAM molecules employed in this study were strategically designed to retain similarity to other molecules used with respect to one of the above principals, yet differ in another key aspect, in order to differentiate cause from correlation (ex. BA-11-PA, 12-PD-PA and DDPA are all similar with respect to alkyl-chain length but have very different surface energy values) (Fig. 3).

This study represents a major advancement in understanding the mechanisms at play between SAMs and linear organic semiconducting molecules. A systematic examination of six self-assembled monolayer structures was carried out to better define the relationship between SAM molecular design and pentacene device performance. High charge carrier mobility pentacene OFET devices are demonstrated utilizing self-assembly to promote favorable pentacene nucleation and growth. Charge carrier mobilities of > 4.0 cm^2 V^{-1} s^{-1} are observed for less ordered molecular SAM structures with non-bulky methyl-/phenyl- terminal groups and alkyl chains of ~$(CH_2)_{12}$. The relationship between SAM surface homogeneity and pentacene device performance is probed using NEXAFS, contact angle goniometry and atomic force microscopy. It is concluded that if a SAM promotes a homogenous liquid-like surface with uninterrupted periodicity, achieved here through the use of mid-length alkyl- phenyl and methyl structures, pentacene device performance will be optimized. However, terminal group should be carefully chosen to still allow for a molecularly smooth surface that does not disrupt surface homogeneity. To further validate this conclusion, a triptycene-terminated phosphonic acid molecule with a short alkyl chain was synthesized. Due to the ridged "pronged" nature of the triptycene moiety, surface homogeneity is never preserved regardless of terminal group orientation, and molecular valleys and peaks are formed after dense assembly. Accordingly, pentacene device performance on this SAM surface is greatly impeded.

A variety of SAM structures with a wide range of surface energies were used in this study, and surface energy was examined with respect to pentacene device performance. It was found that surface energy tends to be a negligible factor in device performance provided that the aforementioned conditions for surface homogeneity are

met. This is promising for realizing integration of organic semiconductor devices into mass production, as the mid-level surface energy of phenyl-terminated amorphous SAM structures could potentially provide the platform for reproducible solution processing of high-performance OFETs.

(a)

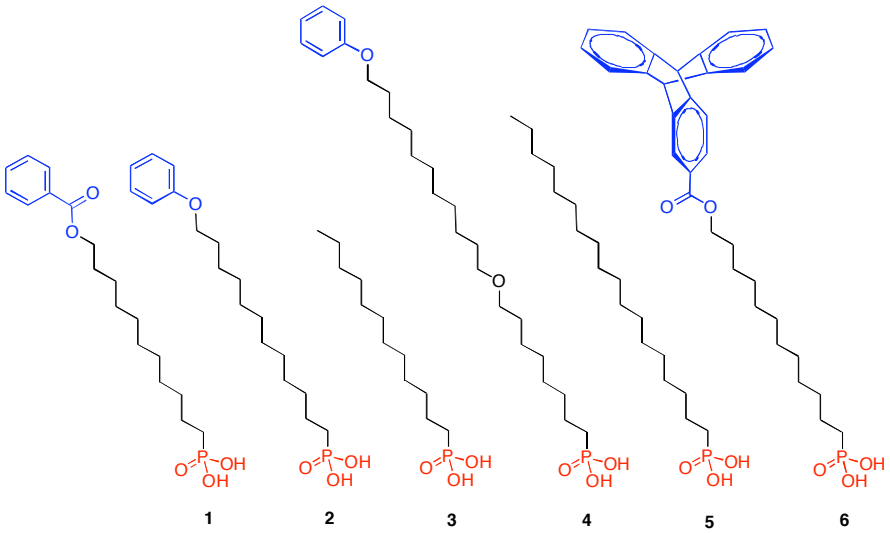

(b)

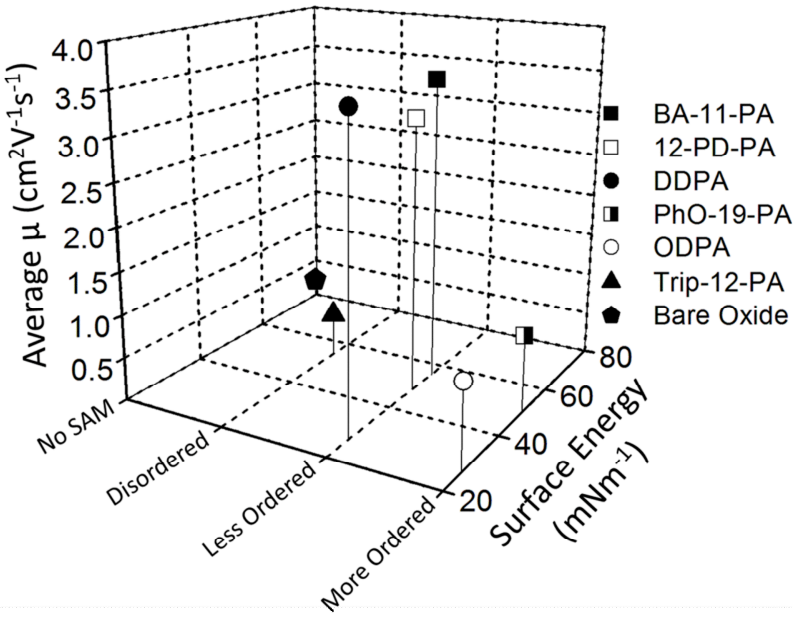

Fig. 3. (a) Molecular structures of all six SAMs. 1) Benzoic acid 11-phosphono-undecyl ester (BA-11-PA), 2) (12-Phenoxy-dodecyl)-phosphonic acid (12-PD-PA), 3) Dodecyl-phosphonic acid (DDPA), 4) [8-(11-Phenoxy-undecyloxy)-octyl]-phosphonic acid (PhO-19-PA), 5) Octadecyl-phosphonic acid (ODPA), and 6) 12-(2-triptycenylcarboxy)dodecylphosphonic acid (Trip-12-PA). (b) Plot of surface energy (X-axis), SAM alkyl-chain order established by dichroic ratio (Y-axis), and charge carrier mobility of pentacene OFET device (Z-axis) of all six SAM structures and bare AlO_x/SiO_2.

4. Low operational voltage and high performance organic field effect memory transistors with solution processed graphene oxide charge storage media

In order to achieve low voltage organic memory transistors an appropriate dielectric and charge trapping layer need to be selected. The operational voltage of an organic transistor can be modulated by controlling the total dielectric thickness (*d*) and dielectric constant (*k*). Research into low voltage platforms for organic transistors is varied and several suitable dielectric systems such as high-*k* transition metal oxides (TMO), ion-gels, and hybrid systems using a stacked self-assembled monolayer (SAM) and an ultrathin high-*k* TMO layer have been studied. In particular, hybrid gate dielectrics have exhibited excellent dielectric properties due to both high accumulation of charges on the dielectric surface and the ability to control the surface energy via a SAM which enables the use of solution processed organic semiconductors. Additionally, the SAM serves to screen the relatively unstable charge distribution of the high-*k* TMO. The molecular structure of SAMs can also be designed to have less leakage current and higher or lower surface energy by adjusting length of molecule and end functional groups. Due to these properties, hybrid dielectrics are a promising platform for low voltage organic memory transistors. Another important component for organic memory transistor is the charge-trapping layer which is generally employed between the gate and tunneling dielectric layers. From a processability and cost-efficiency point of view, graphene oxide is an exemplary candidate for next generation charge trapping layers in organic memory transistors. Key advantages of graphene oxide is that it is well dispersed in water-based solvents and has many charge trapping sites due to structural defects and the presence of hydroxyl and carboxyl groups.

We have demonstrated low voltage organic field effect memory transistors by employing a hybrid gate dielectric and a solution processable graphene oxide charge trap layer (Fig. 4). The hybrid gate dielectric is composed of aluminum oxide (AlOx) and [8-(11-phenoxyundecyloxy)-octyl]phosphonic acid (PhO-19-PA) SAM which successfully blocked leakage current from the gate electrode and provided a suitable surface energy for uniform spin-casting of a graphene oxide (GO) solution. Under an applied gate bias from 4 V to -5 V, low voltage organic memory transistors with a device architecture of Au/Pentacene/PMMA/GO/PhO-19-PA/AlOx/Al showed large hysteresis with a memory window of around 2 V. The amount of stored charge within the GO charge trap layer was determined to be 2.9 x 10^{12} cm^{-2}. The low voltage memory transistors showed an increasing memory window (V_{th} shift) as V_{gs} was incremented while its duration was held constant. Additionally, V_{th} also increasingly shifted positive as V_{gs} was held constant but duration help was incremented. These devices were further characterized and found to work well under repeated write/read/erase/read (W–R–E–R) cycles. Furthermore, our memory transistors showed excellent memory state retention characteristics and are expected to maintain their state for more than one year.

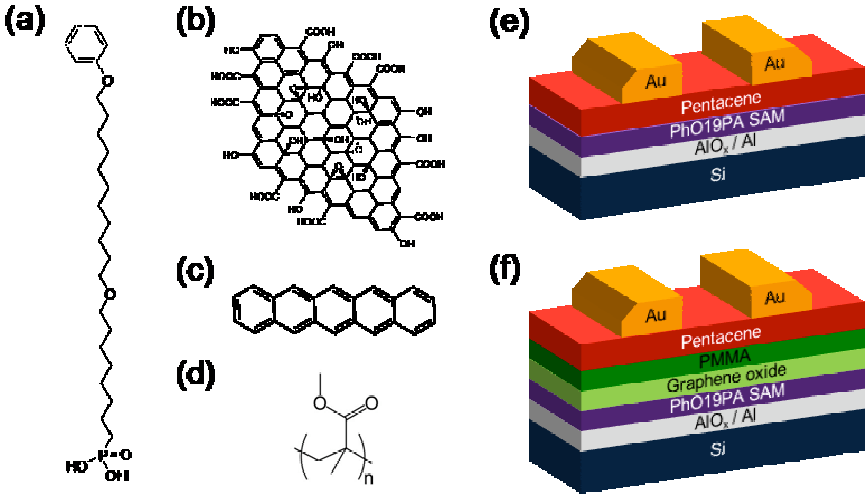

Fig. 4. Chemical structures of (a) [8-(11-phenoxy-undecyloxy)-octyl]phosphonic acid (PhO-19-PA), (b) graphene oxide sheets prepared by a modified Hummer's method, (c) pentacene and (d) poly(methylmethacrylate) (PMMA). Device structures of (e) reference transistor and (f) memory transistor.

5. Systematic doping control of CVD graphene transistors with functionalized self-assembled monolayers

Recent reports have shown it is possible to modulate the properties of graphene by modifying the underlying dielectric surface with a SAM resulting in doping control without compromising the intrinsic graphene performance. However, these studies use exfoliated graphene rather than the more commercially viable CVD-based graphene. In addition, exfoliation severely limits the ability to do a systematic and statistical study based on multiple devices due to the taxing processing steps necessary to fabricate individual devices. In order to circumvent this issue, characterization of these devices is mainly attributed to multiple Raman scans on a few pieces of modified graphene rather than multiple pieces of graphene. While such methodology is useful for obtaining an overall picture of the graphene doping environment it makes it difficult to understand the exact relationship between SAMs and graphene. SAMs are commonly used in organic field-effect transistors to modify the work function of metal electrodes, quench charge trap sites at the interface between semiconductor and metal or dielectric, and modulate the position of the threshold voltage. SAMs represent an ideal platform for control of graphene electronics as they can be designed and functionalized at the molecular scale to cater to specific device requirements. However, there is still a need for better understanding of how SAM-treated dielectrics modulate the doping of graphene devices. In particular, an understanding of how the SAM dipole, while taking into account metal electrode effects, influences graphene has yet to be studied.

We have utilized SAMs with varying dipole magnitudes/directions and directly correlate these values to changes in performance seen in graphene transistors (Fig. 5). It is found that by knowing the z-component of the SAM dipole one can reliably predict the shift in graphene charge neutrality point after taking into account the influence of the metal electrodes (which also play a role in doping graphene). We verify this relationship through density functional theory and comprehensive device studies utilizing atomic force microscopy, x-ray photoelectron spectroscopy, Raman spectroscopy, and electrical characterization of graphene transistors. It is shown that properties of graphene transistors can be predictably controlled with SAMs when considering the total doping environment. Additionally, we find that methylthio-terminated SAMs strongly interact with graphene allowing for a cleaner graphene transfer and enhanced charge mobility. This is crucial for future applications and may enable predictable and controlled band-gap opening of bilayer graphene without the need for a dual gate architecture via self-assembled monolayers.

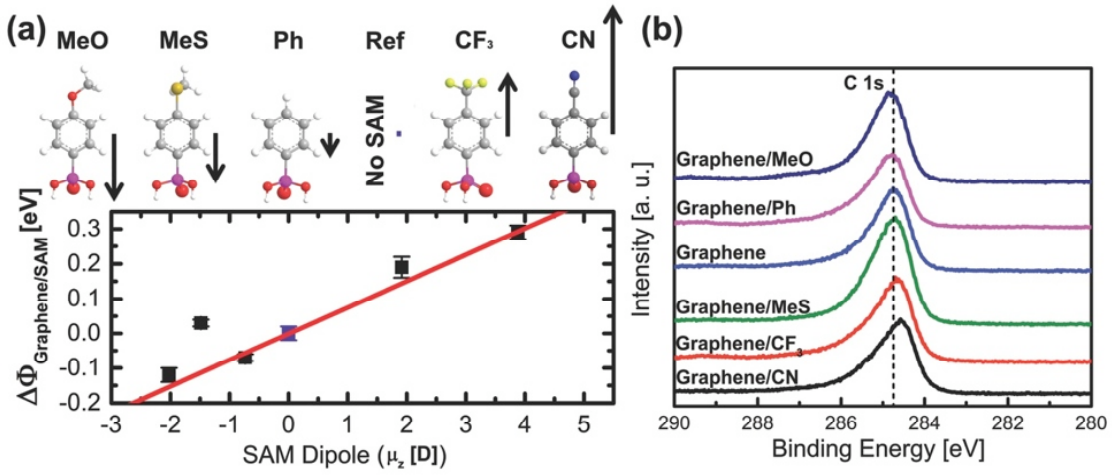

Fig. 5. (a) Visual representation of predicted z-component of SAM dipole (μ_z). Change in graphene/SAM work function as measured by XPS with respect to μ_z. The outlier of the linear fit is the MeS SAM which displays a strong interaction with graphene. (b) C 1s binding energy peak for various graphene/SAMs used in this study. Direct correlation between peak position and SAM dipole is observed.

We have also demonstrated that the chosen SAM binding group can make a significant doping contribution to the properties of graphene transistors (Fig. 6). In particular, phosphonic acid based SAMs intrinsically n-doped graphene transistors. Additionally, we found that when using alkyl-based molecules a SAM with a greater packing density has a stronger doping effect either due to increased dopant density or a reduction in charge trap states. Conversely, we found that silane based SAM molecules do not significantly dope graphene transistors due to their similarity to the underlying dielectric layer. Furthermore, we have shown no significant difference between specific

SAM binding groups used in terms of the extrinsic charge mobility of graphene transistors. Rather, it was found that the packing density and crystallinity of the molecular monolayer plays a key role in enhancing charge mobility once extrinsic factors such as absorbed impurities are removed.

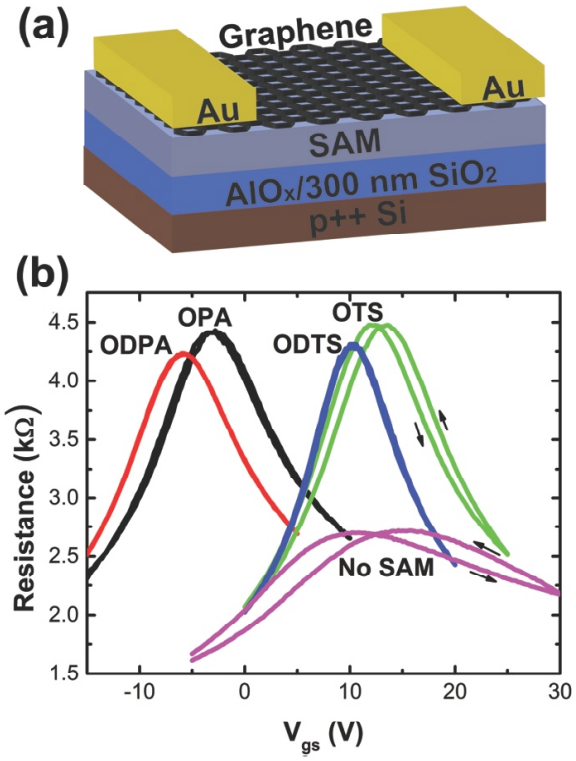

Fig. 6. (a) Schematic of graphene transistors fabricated. Transistors had a channel width 1000 μm and channel lengths of 12, 20, 30, 50, 80, and 100 μm. (b) Representative transfer curves of graphene transistors with SAM on dielectric surface modification compared to an untreated (No SAM) dielectric graphene transistor.

Section 2: Electric Field Assisted Self-Assembly of Organic Nonlinear Optic Materials Through Conformal and Detachable Pyroelectric Elements

Executive Summary

We have explored key strategies of using electric field generated by pyroelectricity to efficiently pole highly efficient OEO materials in thin films and nanophotonic waveguides. Through surface modification, novel pyroelectric elements such as pyroelectric crystals and ceramics are modified as conformal and detachable electric field source to study basic electrostatics and develop new device concepts for hybrid OEO nanophotonic platforms. EO polymers have been processed at multiple length scales and be used in complex and densely packed structures of nano-photonic and plasmonic waveguides to enable ultra-compact, low-power, and high-speed E-O modulators. The study opens up new processing strategies for developing functional dielectrics and their hybrid systems over multi-length scales and dimensions for a broad spectrum of electronic and photonic applications.

1. Pyroelectric poling of EO polymers in multilayered thin films

We conceptualized that pyroelectric crystals and epitaxial films provide an excellent platform for studying poling protocols and self-assembly of organic electro-optic (EO) materials. Table 1 compares the characteristics, strengths and weaknesses of different poling techniques. Although contact and corona poling protocols are quite well established for decades, there do exist some challenging problems. In contact poling, severe charge injection from metal electrodes often results in large current that causes dielectric breakdown of films. Corona poling has difficulty to control the homogeneity of poling fields, and also tends to create surface damage on poled films due to various reactive (such as ozone or nitrogen oxides) and energetic species from corona discharge. These problems

can strongly inhibit the efficient poling and large-scale integration of EO polymers and other polar dielectric materials for device applications. Our research of pyroelectric poling, however, laid the groundwork for using pyroelectric elements as reliable conformal and detachable electric field source to achieve efficient poling of EO polymers and overcoming some of challenges aforementioned.

Table 1. Comparing different poling techniques for the processing of EO polymers.

	Contact Poling	Corona Poling	Pyroelectric Poling
Field strength	1 to 2 MV/cm (voltage source needed)	2 to 5 MV/cm (high voltage source needed)	1 to 4 MV/cm (no voltage source needed thus operationally safe and cost-effective)
Metallization?	Yes for both top and bottom electrodes	Bottom electrode needed	Optional (poled films in all-dielectric structures possible)
Leakage currents	High	Low	Very Low
Thickness range	1-5 μm but difficult for sub-micron or thick films	OK for micron-thick films	0.2 to 5 μm (possible for >50 μm thick films too)
Typical poled area	0.1 to 0.2 cm^2	~ 1-2 cm^2	Pertaining to the size of pyroelectric elements (up to wafer scale)
Poling of multi-layer structures	Highly sensitive to the use of cladding materials	Relatively sensitive to the cladding materials	Less sensitive to the cladding materials (capacitor model)
Poling-induced optical loss	could be high due to high leakage currents	could be high due to surface damage	Low or negligible

A simplified bilayer structure is used for the electrostatics analysis. Fig. 7 shows the schematic drawing of a bilayer laminate comprising a pyroelectric crystal and a dielectric film, where the dielectric film is deposited onto the Z^+ face surface of the crystal. This system can be considered as two capacitors in parallel, and the dielectric film is the recipient medium of pyroelectric fields. Under the equilibrium condition (Fig. 1A), the bulk P_s is fully compensated by the surface σ_{sc}, therefore, there is no electric field within the laminate. However, the temperature change will alter the ionic and electronic forces within the bulk crystal and cause the spontaneous polarization change (ΔP_s). This change can be described as $\Delta P_s = \gamma \Delta T$, where γ is the pyroelectric coefficient of the crystal and ΔT is the change of temperature. When the temperature change is fast enough (0.2 to 0.5 °C/s), there is not enough time for charge compensation to occur, leading to uncompensated charges of ΔP_s in the form of excessive polarization charges (Fig. 1B) or screening charges (Fig. 1C). These "static" charges are the origin of electric field (E_{di}) creation inside the dielectric medium. If the loss of pyroelectric charges is negligibly small, it would yield

$$E_{di} = \gamma \Delta T / [\varepsilon_0 (\varepsilon_{di} + \varepsilon_{cr} L_{di} / L_{cr})] \quad (1)$$

where ε_0, ε_{cr}, and ε_{di} are the dielectric permittivities of free space, the pyroelectric crystal and the dielectric film, respectively. L_{cr} and L_{di} are the thickness of the crystal along the polar axis and the dielectric film, respectively.

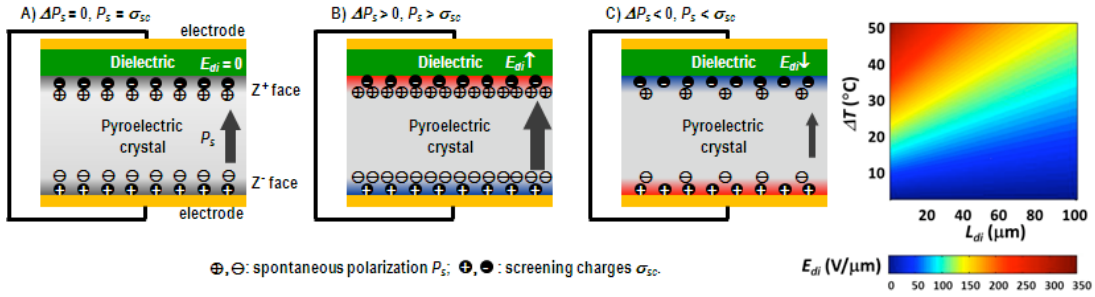

Fig. 7. The bilayer laminate comprises a pyroelectric crystal and a dielectric thin film (such as EO polymer) on the Z^+ face surface of the crystal. The large closed arrows in the layer of pyroelectric crystal denote the spontaneous polarization (P_s) of pyroelectric crystals, and the thickness and length of the arrows indicate relative magnitude of P_s at different temperatures. The generation of uncompensated charges (ΔP_s) through the pyroelectric effect is the source of electric field (E_{di}) in the dielectric thin film, and the small open arrows at the thin layer of dielectrics represent the direction

In this idealized model, a modest temperature change (10 to 50 °C) will lead to a considerably large electrostatic field in a thin film dielectric material. If the ε_{di} of a typical amorphous organic thin film dielectrics is assumed to be 3.0, the maximum achievable potential on the charged surface can be as high as 15 kV, and the effective field strength in the dielectric films can vary from 50 to 350 V/mm over a broad range of thickness (from sub-micron to 100 mm).

Fig. 8 illustrates the schematic design of forming the multi-layerered pyroelectric/OEO laminate for standalone EO characterization, where the contact between them is conformal and detachable. Such a soft lamination by using spin-on PDMS is highly desirable for pyroelectric poling, and the polymer film and the pyroelectric element can be separated from each other after the processing. This approach provided great convenience for both linear optical and EO characterization of samples. It has also established useful database for guiding the electrostatic analysis of the pyroelectric/OEO systems, identified the key electrical /thermal parameters, and defined the spatial distribution in both transverse and quasi-longitudinal configuration through rational design of dielectric/electrical hetero-structures. Upon rapid cooling of the pyroelectrics/EO polymer laminate from its equilibrated condition at elevated temperature, EO polymer films can be effectively poled by the pyroelectric crystals without the use of external DC voltage source, and the EO coefficients of stand-alone poled films are currently at the level of 80–150 pm/V.

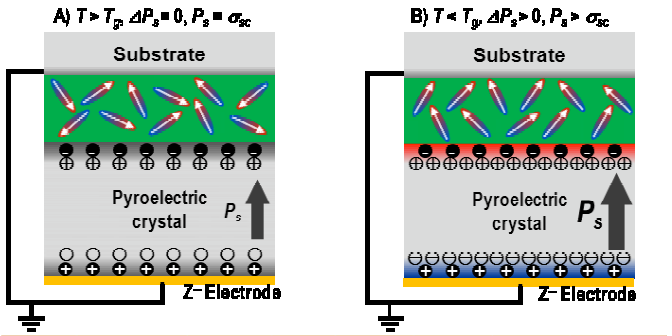

Sample Entries	Chromophore loading	Pyro-Element	ΔT (°C)	r_{33} (pm/V)	E_{equiv} (V/μm)	E_{theo} (V/μm)	E_{equiv}/E_{theo} (×100%)
1	15wt%	LT	15	**60**	67	75	**89%**
2		LT	20	**81**	90	99	**91%**
3		LT	25	**78**	87	124	**70%**
4		LT	15	**58**	64	75	**85%**
5		LT	20	**78**	87	99	**88%**
7		LN	20	**42**	47	47	**100%**
8		PZT	60	**108**	120	–	–
9	25wt%	PZT	60	**130**	112	–	–
10	33wt%	PZT	60	**150**	94	–	–

Fig. 8. Top: Schematic drawings of multi-layered structures for pyroelectric poling of guest-host E-O polymers in the parallel-plate (transverse) design: A) unpoled films; B) poled films. **Bottom**: Summary of thin film poling results.

2. Pyroelectric poling of hybrid silicon EO polymer slot waveguide ring resonator modulators

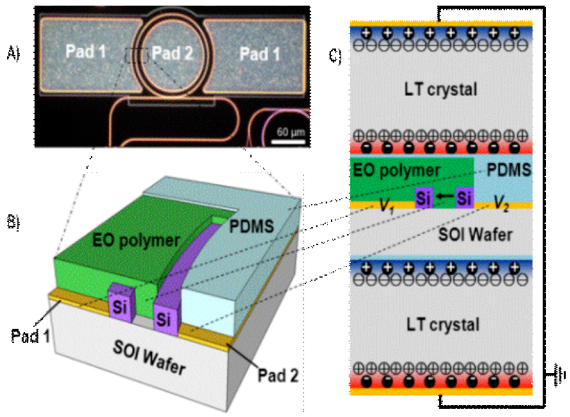

Fig. 9. Design of heterogeneous dielectric structures to create the in-plane polarization for efficient pyroelectric poling. A: Dark field optical micrograph of slot waveguide ring resonator; B: the partial cutaway view illustration of heterogeneous dielectric structures.

The pyroelectric poling protocol can also induce a strong in-plane poling of EO polymer in hybrid silicon slot waveguides. In the design shown in Fig. 9, the potential on electrode pad **1** and **2** can be calculated respectively by integrating the electric field strength from the ground, which is determined by the $\Delta\varepsilon_{di}$ and related parameters of heterogeneous dielectric structures. It can be estimated that the potential difference between two pads be at the level of a few tenth volts with micron thick dielectric (EO polymer and PDMS) layer, corresponding to a strong in-plane electric field up to 100 to 200 V/mm across a 200 nm silicon slot. This level of field strength is sufficient to direct the noncentrosymmetric assembly and orientational polarization of OEO materials.

The pyroelectric poling of EO polymers in slot waveguides led to a record-high tunability of resonance wavelength shift (25 pm/V) in ring-resonator modulators with a 6 dB bandwidth of 1 GHz. This result is 60% higher than those obtained from contact-poled devices, and it exceeds the best value reported for depletion-based silicon

ring modulators. The dynamic dissipations $(1/4)CV^2$ for this new ring resonator is around 30 fJ, based on an estimated capacitance of ~27 fF and a drive voltage of 2V swing. The energy consumption of this device compares also favorably to other state-of-the-art semiconductor optical modulators for low-power interconnect applications such as electro-absorptive devices using GeSi (25 fJ) or Ge (100 fJ), but without the bandwidth limitation.

3. Spontaneously poling of electro-optic polymer thin films across a 1.1-mm thick glass substrate by pyroelectric crystals

We have demonstrated a method to efficiently pole EO polymers using pyroelectric crystals from outside of a thick insulating substrate, with testing electrodes left floating during the whole poling process (Fig. 10). The electric potential generated from such pyroelectric crystals during poling were estimated to be at the level of several tens of kilovolts, leading to high electric fields of $7\text{x}10^7$ V/m to the EO layer, large r_{33}s of up to 62 pm/V at 1300 nm, and three orders magnitude lower LTC during poling. The good agreement between theory and experimentally measured results in the study provide important insights of electrostatics in pyroelectric systems and their effective interactions with thin film EO polymeric materials. It also demonstrates that pyroelectric poling is a promising alternative to commonly used contact poling and corona poling that offers unique advantages of high field strength and near-zero LTC for polarizing dielectric functional materials and devices.

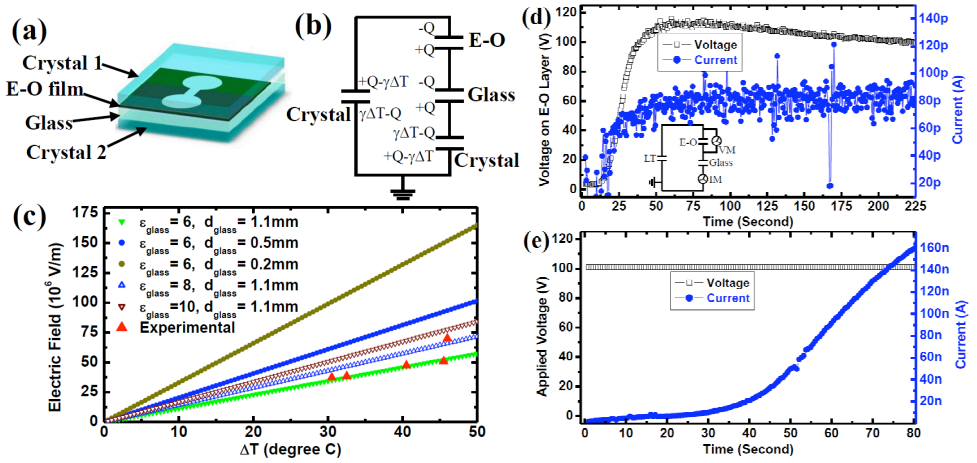

Fig. 10. (a) Structure and (b) Equivalent circuit of multiple capacitors for the pyroelectric poling of this study. (c) Theoretical electric field calculated on different insulating substrates by using ε_{EO} of 3.5, ε_{cr} of 43 and γ of 176 $\mu C \cdot m^{-2} \cdot K^{-1}$ for LT crystal. Monitoring the LTC and voltage of E-O thin films by (d) pyroelectric poling (inset, the circuit of multiple layer capacitors for the *in-situ* measurement); (e) contact poling.

4. Systematically analyze electrostatics models to quantify electric field generation from commonly used pyroelectric elements

A general electrostatic model, namely capacitor-resistor model has been developed to analyze the effective electric field generation of PZT or LT to thin film dielectrics. In this model, the pyroelectric element behaves as a current generator in parallel with its own resistance (R_{pyro}) and capacitance (C_{pyro}). The voltage resulting from a change in temperature is applied to EO polymer films which can be represented by a capacitor (C_{EO}) and a resistor (R_{EO}) (Fig. 11).

As opposed to the capacitor-only model that is an idealized model for simple estimation, this new capacitor-resistor model considers nearly all the basic experimental parameters that can affect the field strength and leakage current of pyroelectric poling, including the area/thickness factor, the temperature change, the heating/cooling rate, the pyroelectric coefficients, dielectric constants, and the electrical resistivities of materials. It agrees well with our experimental results in using PZT or LT to pole highly efficient EO polymers. As shown in Fig. 12 and Fig. 13, a modest temperature change (50 °C to 100 °C) in a LT or PZT will lead to a very large electrostatic field in a

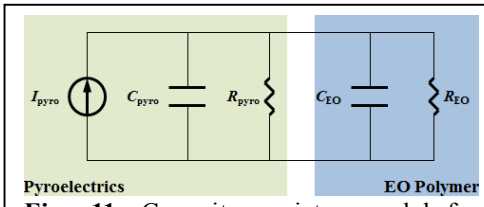

Fig. 11. Capacitor-resistor model for pyroelectric poling of EO polymers

thin film dielectric material. The maximum achievable field strengths in micron-thick EO polymers films are ~200 V/mm for LT, and ~400 V/mm for PZT, and further changing the area/thickness factors can also considerably increase the achievable field strength to the level of 1000 V/mm. The larger achievable field strength from PZT is mainly due to its large pyroelectric coefficients. This level of static electric field is adequate to align the dipoles of NLO chromophores or polarize other dielectric materials.

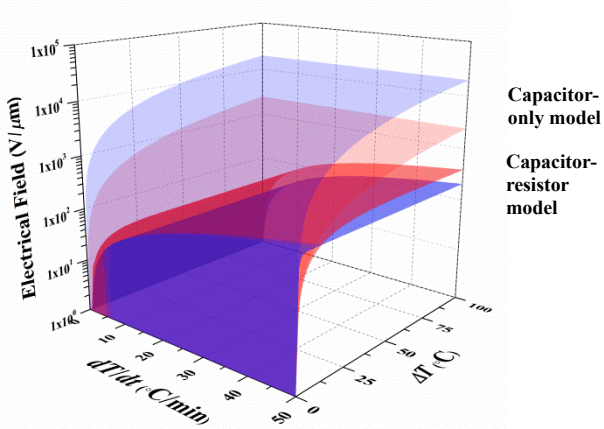

Fig. 12. Electric field generation during pyroelectric poling of thin film EO polymers as a function of temperature change (ΔT) and the heating rate of pyroelectric elements. **Blue**: pyroelectric field by **$LiTaO_3$**; **Red**: pyroelectric field by **PZT**.

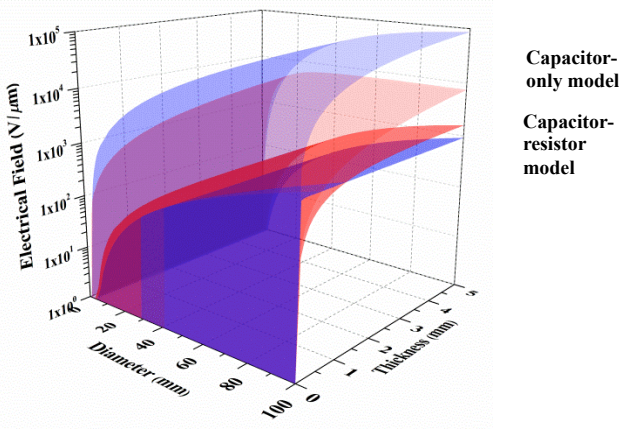

Fig. 13. Electric field generation during pyroelectric poling of thin film EO polymers as a function of areas and thicknesses for pyroelectric elements. **Blue**: pyroelectric field by **$LiTaO_3$**; **Red**: pyroelectric field by **PZT**.

A two-hotplate pyroelectric EO poling was experimentally examined by LT and PZT based on the desirable conditions concluded from the modeling analysis. The temperature change rate dT/dt is set to be the highest rate of 20°C/min that the hotplate in our lab can handle. The temperature change window ΔT is chosen as 60°C to guarantee a long enough operational time of 3min. PZT in disk shape with 30mm-diameter surface and 1mm thickness are selected to perform the poling.

The EO materials chosen in these particular poling experiments are that **AJLZ53** chromophores were solved in 350K molecular weight PMMA, P(MMA-St) or COPS at weight percent of 15%, 25% or 35%. A thin PVP (~150nm) film was first deposited onto an ITO substrate. The EO solution was then spin-coated onto it to form an EO layer at the thickness between 1 μm to 2 μm. The samples were spin-coated again with a thin PVP film (~150nm) on the top. Therefore, a thin film of three-layered structures with EO sandwiched between PVPs was prepared (shown in Fig. 14). PVPs work as barrier layers to effectively prevent the charge injection into the EO layer so that the charge induced localized environment change is minimized during the poling. Typically more than one order enhancement of EO resistivity was observed for our AJLZ53 EO materials with barrier layers. All prepared samples were baked at 65°C in vacuum oven for 12 hours to evaporate the solvents. After that, the top electrode was patterned using Au plasma sputtering through a round mask with a diameter of ~3.6mm.

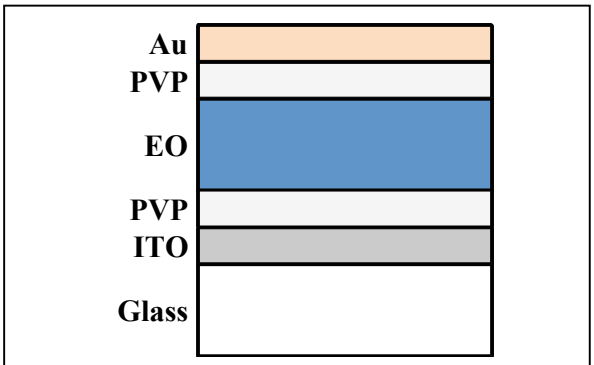

Fig. 14. *Structure of EO samples. Not to scale.*

After the pyro-poling, EO coefficient r_{33} was measured using simple Teng-Man reflection method. A simple normalization to correct potential drop over PVPs layers was applied and the final results are listed in Table . The effective electrical field was estimated based on the linear proportion of r_{33} value compared to the contact poling using the electrical field of 100V/μm. The electrical field estimated in capacitor-resistor model is close to the values observed in experiments.

Table 2 . List of experimental pyro-poling results by using PZT

EO material	Pyroelectric material	Normalized r_{33} (pm/V) @ 1.31 μm	Effective electrical field (V/μm)
AJLZ53 (15%) in PMMA	PZT	86	120
AJLZ53 (25%) in P(MMA-ST)	PZT	120	112
AJLZ53 (35%) in COPS	PZT	137	94

In summary, a simple and practical two-hotplates approach was proposed for pyroelectric poling. Comparing to a capacitor-only model, the quantitative analysis based on capacitor-resistor model provides us a deep insight into this unique poling method. PZT exhibits higher performance in generating electrical field than LT. The theory guided optimization of experimental parameters maximized the final poling efficiency. A 120% poling efficiency was already observed using available PZT with 30mm-diameter surface and 1mm thickness under a mild poling condition. Further enhancement can be made by enlarging PZT's dimension and improving heating or cooling rates.

Archival publications (published) during reporting period:

1. Cernetic, N., Hutchins, D. O., Ma, H., Jen, A. K.-Y., "Influence of Self-Assembled Monolayer Binding Group on CVD Graphene Transistors", *Appl. Phys. Lett.* **2015**, *106*, 021603.
2. Cernetic, N., Wu, S. F., Davies, J. A., Krueger, B. W., Hutchins, D. O., Xu, X. D., Ma, H., Jen, A. K.-Y., "Systematic Doping Control of CVD Graphene Transistors with Functionalized Aromatic Self-Assembled Monolayers", *Adv. Func. Mater.* **2014**, *24*, 3464-3470.
3. Kim, T. W., Cernetic, N., Gao, Y., Bae, S., Ma, H., Chen, H. Z., Jen, A. K.-Y., "Low Operational Voltage and High Performance Organic Field Effect Memory Transistor with Solution Processed Graphene Oxide Charge Storage Media", *Org. Ele.* **2014**, *15*, 2775-2782.
4. Tucker, N. M., Briseno, A. L., Acton, O., Yip, H. L., Ma, H., Jenekhe, S. A., Xia, Y. N., Jen, A. K.-Y., "Solvent-Dispersed Benzothiadiazole-Tetrathiafulvalene Single-Crystal Nanowires and Their Application in Field-Effect Transistors", *ACS Appl. Mater. Interface* **2013**, *5*, 2320.
5. Hutchins, D. O., Weidner, T., Baio, J., Polishak, B., Acton, O., Cernetic, N., Ma, H, Jen, A. K.-Y., "Effect of Self-Assembled Monolayer Structural Order, Surface Homogeneity and Surface Energy on Pentacene Morphology and Thin Film Transistor Device Performance", *J. Mater. Chem. C.*, **2013**, *1(1)*, 101. **(A Most Accessed Manuscript for 2013)**
6. Cernetic, N., Acton, O., Weidner, T., Hutchins, D. O., Baio, J. E., Ma, H., Jen, A. K.-Y. "Bottom-Contact Small-Molecule n-Type Organic Field Effect Transistors Achieved via Simultaneous Modification of Electrode and Dielectric Surfaces with Enhanced Performance Comparable to Top-Contact Architecture", *Org. Ele.* **2012**, *13*, 3226.
7. Hutchins, D. O., Acton, O., Weidner, T., Cernetic, N., Baio, J. E., Ting, G., Castner, D. G., Ma, H., Jen, A. K.-Y., "Solid-State Densification of Spun-Cast Self-Assembled Monolayers for Use in Ultra-Thin Hybrid Dielectrics", *Appl. Surface Sci.* **2012**, *261*, 908.
8. Ma, H., Acton, O., Hutchins, D. O., Cernetic, N., Jen, A. K.-Y., "Multifunctional Phosphonic Acid Self-Assembled Monolayers on Metal Oxides as Dielectrics, Interface Modification Layers and Semiconductors for Low-Voltage High-Performance Organic Field-Effect Transistors", *Phys. Chem. Chem. Phys.* **2012**, *14*, 14110. **(Featured on Front Cover, invited feature article).**
9. Kim, T. W., Zeigler, D. F., Acton, O., Yip, H. L., Ma, H., Jen, A. K.-Y., "All-Organic Photopatterned One Diode-One Resistor Cell Array for Advanced Organic Nonvolatile Memory Applications", *Adv. Mater.* **2012**, *24*, 828. **(Featured on Front Cover).**
10. Li, M.; Huang, S.; Zhou, X.-H.; Zang, Y.; Wu, J.; Cui, Z.; Luo, J., Jen, A. K.-Y., "Poling Efficiency Enhancement of Tethered Binary Nonlinear Optical Chromophores for Achieving Ultrahigh n^3r_{33} Figure-of-Merit of 2601 pm/V" *J. Mater. Chem. C* **2015**, In Press.
11. Park, D. H.; Pagan, V. R.; Murphy, T. E.; Luo, J.; Jen, A. K.-Y.; Herman, W. N., "Free space millimeter wave-coupled electro-optic high speed nonlinear polymer phase modulator with in-plane slotted patch antennas" *Opt. Express* **2015**, *23*, 9464-9476.
12. Nelson, C. A.; Luo, J.; Jen, A. K.-Y. Jen, Laghumavarapu, R. B.; Huffaker, D. L.; Zhu, X., "Time-, Energy-, and Phase-Resolved Second Harmonic Generation at Semiconductor Interfaces" *J. Phys. Chem. C* **2014**, *118*, 27981-27988.

13. Huang, S.; Luo, J.; Jin, Z.; Li, M.; Kim, T.-D.; Chen, A.; Jen, A. K.-Y., "Spontaneously Poling of Electro-Optic Polymer Thin Films across a 1.1-mm Thick Glass Substrate by Pyroelectric Crystals" *Appl. Phys. Lett.* **2014**, *105*, 183305.
14. Prorok, S.; Petrov, A.; Eich, M.; Luo, J.; Jen, A. K,-Y., "Modification of a Teng-Man Technique to Measure both r33 and r13 Electro-Optic Coefficients" *Appl. Phys. Lett.* **2014**, *105*, 113302.
15. Ren, F.; Wang, X.; Li, Z.; Luo, J.; Jang, S.-H.; Jen, A. K.-Y.; Wang, A. X., "Enhanced Third Harmonic Generation by Organic Materials on High-Q Plasmonic Photonic Crystals" *Opt. Express* **2014**, *22*, 20292-20297.
16. Enami, Y.; Kayaba, Y.; Luo, J.; Jen, A. K.-Y., "Mesoporous Sol-Gel Silica Cladding for Hybrid TiO_2/Electro-Optic Polymer Waveguide Modulators" *Opt. Express* **2014**, *22*, 16418-16423.
17. Zhang, X.; Hosseini, A.; Subbaraman, H.; Wang, S.; Zhan, Q.; Luo, J.; Jen, A. K.-Y.; Chen, R. T., "Integrated Photonic Electromagnetic Field Sensor Based on Broadband Bowtie Antenna Coupled Silicon Organic Hybrid Modulator" *J. Lightwave Technol.* **2014**, *32*, 3774-384.
18. Prorok, S.; Petrov, A.; Eich, M.; Luo, J.; Jen, A. K.-Y., "Configurable Silicon Photonic Crystal Waveguides" *Appl. Phys. Lett.* **2013**, *103*, 261112.
19. Huang, W.; Jin, Z.; Shi, Z.; Intemann, J. J.; Li, M.; Luo, J.; Jen, A. K.-Y., "Spontaneous Thermal Crosslinking of a Sydnonecontaining Side-Chain Polymer with Maleimides through a Vonvergent [3 + 2] Dual Cycloaddition/Cycloreversion Process for Electro-Optics" *Polym. Chem.* **2013**, *4*, 5760-5767.
20. Luo, J.; Jen, A. K.-Y., "Highly Efficient Organic Electrooptic Materials and Their Hybrid Systems for Advanced Photonic Devices" *IEEE J. Sel. Top. Quant.* **2013**, *19*, 3401012.
21. Li, M.; Jin, Z.; Cernetic, N.; Luo, J.; Cui, Z.; Jen, A. K.-Y., "Photo-Induced Denitrogenation of Triazoline Moieties for Efficient Photo-Assisted Poling of Electro-Optic Polymers" *Polym. Chem.* **2013**, *4*, 4434-4441.
22. Intemann, J. J.; Huang, W.; Jin, Z.; Shi, Z.; Yang, X.; Yang, J.; Luo, J.; Jen, A. K.-Y.,"Cascading Retro-Diels–Alder Cycloreversion and Sydnone-Maleimide Based Double 1,3-Dipolar Cycloaddition for Quantitative Thermal Cross-Linking of an Amorphous Polymer Solid" *ACS Macro Lett.* **2013**, *2*, 256-259.

Cumulative lists of people involved in and the research effort.

Nathan Cernetic, graduate student, material processing and OFET characterization (in his 5th year of Ph. D. study)
Li Qiang, graduate student, material processing and OFET characterization (in his 1st year of M.S. study)
Jui-An Li, graduate student, material processing and OFET characterization (M. S. obtained in 2013)
Jordan Quan Tran, undergraduate student, material processing and OFET characterization (B. S. obtained in 2015)
Courtney Chheng, undergraduate student, material processing and OFET characterization (in her 2nd year of B. S. study)
Dr. Hong Ma, research associate professor, material design, synthesis, and processing for OFETs
Dr. Jingdong Luo, research scientist, design, synthesis, and pyroelectric poling of organic EO materials

Changes in research objective, if any: None

Changes in AFOSR program manager, if any: None

Extensions granted or milestones slipped, if any: None

Include any new discoveries, inventions, or patent disclosures during this reporting period (if none, report none): None

1.

1. Report Type

Final Report

Primary Contact E-mail
Contact email if there is a problem with the report.

ajen@u.washington.edu

Primary Contact Phone Number
Contact phone number if there is a problem with the report

206-543-2626

Organization / Institution name

University of Washington

Grant/Contract Title
The full title of the funded effort.

Self Assembly and Pyroelectric Poling for Organics

Grant/Contract Number
AFOSR assigned control number. It must begin with "FA9550" or "F49620" or "FA2386".

FA9550-12-1-0076

Principal Investigator Name
The full name of the principal investigator on the grant or contract.

Alex K.-Y. Jen

Program Manager
The AFOSR Program Manager currently assigned to the award

Dr. Charles Lee

Reporting Period Start Date

04/01/2012

Reporting Period End Date

03/31/2015

Abstract

Insulating, dipolar and semiconducting molecular phosphonic acid (PA) self-assembled monolayers (SAMs) have been developed for applications in organic field-effect transistors (OFETs) and graphene transistors for low-power, low-cost flexible electronics. Multifunctional SAMs on ultrathin metal oxides, such as hafnium oxide and aluminum oxide, are shown to realize (1) enhanced performance of self-assembled monolayer field-effect transistors (SAMFETs) with top-contact geometry through molecular tailoring, heated assembly and thermal annealing, (2) bottom-contact small-molecule n-type organic field effect transistors achieved via simultaneous modification of electrode and dielectric surfaces, (3) understanding of effects from self-assembled monolayer structural order, surface homogeneity and surface energy on pentacene morphology and thin film transistor device performance, (4) low operational voltage and high performance organic field effect memory transistors with solution processed graphene oxide charge storage media, and (5) systematic doping control of CVD graphene transistors with functionalized self-assembled monolayers.

Key strategies of using electric field generated by pyroelectricity have been explored to efficiently pole highly efficient organic electro-optic (OEO) materials in thin films and nanophotonic waveguides. Through surface modification, novel pyroelectric elements such as pyroelectric crystals and ceramics are modified

as conformal and detachable electric field source to study basic electrostatics and develop new device concepts for hybrid OEO nanophotonic platforms. EO polymers have been processed at multiple length scales and be used in complex and densely packed structures of nano-photonic and plasmonic waveguides to enable ultra-compact, low-power, and high-speed E-O modulators. The study opens up new processing strategies for developing functional dielectrics and their hybrid systems over multilength scales and dimensions for a broad spectrum of electronic and photonic applications.

Distribution Statement

This is block 12 on the SF298 form.

Distribution A - Approved for Public Release

Explanation for Distribution Statement

If this is not approved for public release, please provide a short explanation. E.g., contains proprietary information.

SF298 Form

Please attach your SF298 form. A blank SF298 can be found here. Please do not password protect or secure the PDF The maximum file size for an SF298 is 50MB.

Form 298-Jen.pdf

Upload the Report Document. File must be a PDF. Please do not password protect or secure the PDF . The maximum file size for the Report Document is 50MB.

AFOSR-Assembly-Pyro poling.pdf

Upload a Report Document, if any. The maximum file size for the Report Document is 50MB.

Archival Publications (published) during reporting period:

1. Cernetic, N., Hutchins, D. O., Ma, H., Jen, A. K.-Y., “Influence of Self-Assembled Monolayer Binding Group on CVD Graphene Transistors”, Appl. Phys. Lett. 2015, 106, 021603.
2. Cernetic, N., Wu, S. F., Davies, J. A., Krueger, B. W., Hutchins, D. O., Xu, X. D., Ma, H., Jen, A. K.-Y., “Systematic Doping Control of CVD Graphene Transistors with Functionalized Aromatic Self-Assembled Monolayers”, Adv. Func. Mater. 2014, 24, 3464-3470.
3. Kim, T. W., Cernetic, N., Gao, Y., Bae, S., Ma, H., Chen, H. Z., Jen, A. K.-Y., “Low Operational Voltage and High Performance Organic Field Effect Memory Transistor with Solution Processed Graphene Oxide Charge Storage Media”, Org. Ele. 2014, 15, 2775-2782.
4. Tucker, N. M., Briseno, A. L., Acton, O., Yip, H. L., Ma, H., Jenekhe, S. A., Xia, Y. N., Jen, A. K.-Y., “Solvent-Dispersed Benzothiadiazole-Tetrathiafulvalene Single-Crystal Nanowires and Their Application in Field-Effect Transistors”, ACS Appl. Mater. Interface 2013, 5, 2320.
5. Hutchins, D. O., Weidner, T., Baio, J., Polishak, B., Acton, O., Cernetic, N., Ma, H, Jen, A. K.-Y., “Effect of Self-Assembled Monolayer Structural Order, Surface Homogeneity and Surface Energy on Pentacene Morphology and Thin Film Transistor Device Performance”, J. Mater. Chem. C., 2013, 1(1), 101. (A Most Accessed Manuscript for 2013)
6. Cernetic, N., Acton, O., Weidner, T., Hutchins, D. O., Baio, J. E., Ma, H., Jen, A. K.-Y. “Bottom-Contact Small-Molecule n-Type Organic Field Effect Transistors Achieved via Simultaneous Modification of Electrode and Dielectric Surfaces with Enhanced Performance Comparable to Top-Contact Architecture”, Org. Ele. 2012, 13, 3226.
7. Hutchins, D. O., Acton, O., Weidner, T., Cernetic, N., Baio, J. E., Ting, G., Castner, D. G., Ma, H., Jen, A. K.-Y., “Solid-State Densification of Spun-Cast Self-Assembled Monolayers for Use in Ultra-Thin Hybrid Dielectrics”, Appl. Surface Sci. 2012, 261, 908.
8. Ma, H., Acton, O., Hutchins, D. O., Cernetic, N., Jen, A. K.-Y., “Multifunctional Phosphonic Acid Self-Assembled Monolayers on Metal Oxides as Dielectrics, Interface Modification Layers and Semiconductors for Low-Voltage High-Performance Organic Field-Effect Transistors”, Phys. Chem. Chem. Phys. 2012, 14, 14110. (Featured on Front Cover, invited feature article).
9. Kim, T. W., Zeigler, D. F., Acton, O., Yip, H. L., Ma, H., Jen, A. K.-Y., “All-Organic Photopatterned One Diode-One Resistor Cell Array for Advanced Organic Nonvolatile Memory Applications”, Adv. Mater. 2012, 24, 828. (Featured on Front Cover).

10. Li, M.; Huang, S.; Zhou, X.-H.; Zang, Y.; Wu, J.; Cui, Z.; Luo, J., Jen, A. K.-Y., “Poling Efficiency Enhancement of Tethered Binary Nonlinear Optical Chromophores for Achieving Ultrahigh n3r33 Figure-of-Merit of 2601 pm/V” J. Mater. Chem. C 2015, In Press.
11. Park, D. H.; Pagan, V. R.; Murphy, T. E.; Luo, J.; Jen, A. K.-Y.; Herman, W. N., “Free space millimeter wave-coupled electro-optic high speed nonlinear polymer phase modulator with in-plane slotted patch antennas” Opt. Express 2015, 23, 9464-9476.
12. Nelson, C. A.; Luo, J.; Jen, A. K.-Y. Jen, Laghumavarapu, R. B.; Huffaker, D. L.; Zhu, X., “Time-, Energy-, and Phase-Resolved Second Harmonic Generation at Semiconductor Interfaces” J. Phys. Chem. C 2014, 118, 27981-27988.
13. Huang, S.; Luo, J.; Jin, Z.; Li, M.; Kim, T.-D.; Chen, A.; Jen, A. K.-Y., “Spontaneously Poling of Electro-Optic Polymer Thin Films across a 1.1-mm Thick Glass Substrate by Pyroelectric Crystals” Appl. Phys. Lett. 2014, 105, 183305.
14. Prorok, S.; Petrov, A.; Eich, M.; Luo, J.; Jen, A. K,-Y., “Modification of a Teng-Man Technique to Measure both r33 and r13 Electro-Optic Coefficients” Appl. Phys. Lett. 2014, 105, 113302.
15. Ren, F.; Wang, X.; Li, Z.; Luo, J.; Jang, S.-H.; Jen, A. K.-Y.; Wang, A. X., “Enhanced Third Harmonic Generation by Organic Materials on High-Q Plasmonic Photonic Crystals” Opt. Express 2014, 22, 20292-20297.
16. Enami, Y.; Kayaba, Y.; Luo, J.; Jen, A. K.-Y., “Mesoporous Sol-Gel Silica Cladding for Hybrid TiO2/Electro-Optic Polymer Waveguide Modulators” Opt. Express 2014, 22, 16418-16423.
17. Zhang, X.; Hosseini, A.; Subbaraman, H.; Wang, S.; Zhan, Q.; Luo, J.; Jen, A. K.-Y.; Chen, R. T., “Integrated Photonic Electromagnetic Field Sensor Based on Broadband Bowtie Antenna Coupled Silicon Organic Hybrid Modulator” J. Lightwave Technol. 2014, 32, 3774-384.
18. Prorok, S.; Petrov, A.; Eich, M.; Luo, J.; Jen, A. K.-Y., “Configurable Silicon Photonic Crystal Waveguides” Appl. Phys. Lett. 2013, 103, 261112.
19. Huang, W.; Jin, Z.; Shi, Z.; Intemann, J. J.; Li, M.; Luo, J.; Jen, A. K.-Y., “Spontaneous Thermal Crosslinking of a Sydnonecontaining Side-Chain Polymer with Maleimides through a Vonvergent [3 + 2] Dual Cycloaddition/Cycloreversion Process for Electro-Optics” Polym. Chem. 2013, 4, 5760-5767.
20. Luo, J.; Jen, A. K.-Y., “Highly Efficient Organic Electrooptic Materials and Their Hybrid Systems for Advanced Photonic Devices” IEEE J. Sel. Top. Quant. 2013, 19, 3401012.
21. Li, M.; Jin, Z.; Cernetic, N.; Luo, J.; Cui, Z.; Jen, A. K.-Y., “Photo-Induced Denitrogenation of Triazoline Moieties for Efficient Photo-Assisted Poling of Electro-Optic Polymers” Polym. Chem. 2013, 4, 4434-4441.
22. Intemann, J. J.; Huang, W.; Jin, Z.; Shi, Z.; Yang, X.; Yang, J.; Luo, J.; Jen, A. K.-Y.,“Cascading Retro-Diels–Alder Cycloreversion and Sydnone-Maleimide Based Double 1,3-Dipolar Cycloaddition for Quantitative Thermal Cross-Linking of an Amorphous Polymer Solid” ACS Macro Lett. 2013, 2, 256-259.

Changes in research objectives (if any):

None

Change in AFOSR Program Manager, if any:

None

Extensions granted or milestones slipped, if any:

None

AFOSR LRIR Number

LRIR Title

Reporting Period

Laboratory Task Manager

Program Officer

Research Objectives

Technical Summary

Funding Summary by Cost Category (by FY, $K)

	Starting FY	FY+1	FY+2
Salary			
Equipment/Facilities			
Supplies			
Total			

Report Document

Report Document - Text Analysis

Report Document - Text Analysis

Appendix Documents

2. Thank You

E-mail user

Jun 17, 2015 17:43:15 Success: Email Sent to: ajen@u.washington.edu